

REMOVAL OF THIN CIRRUS PATH RADIANCES IN THE 0.4 - 1.0 μm SPECTRAL REGION USING THE 1.375- μm STRONG WATER VAPOR ABSORPTION CHANNEL

Bo-Cai Gao¹, Yoram J. Kaufman², Wei Han³, and Warren J. Wiscombe²

¹Remote Sensing Division, Code 7212, Naval Research Laboratory, Washington, DC 20375

²Climate and Radiation Branch, Code 913, NASA Goddard Space Flight Center, Greenbelt, MD 20771

³SFA, Inc., Largo, MD 20774

1. INTRODUCTION

Through analysis of spectral imaging data acquired with the Airborne Visible Infrared Imaging Spectrometer (AVIRIS) (Vane et al., 1993) from an ER-2 aircraft at 20 km altitude during several field programs, it was found that narrow channels near the center of the strong 1.38- μm water vapor band are very sensitive in detecting thin cirrus clouds. Based on this observation from AVIRIS data, a channel centered at 1.375 μm with a width of 30 nm was selected for the Moderate Resolution Imaging Spectrometer (MODIS) for remote sensing of cirrus clouds from space. The sensitivity of the 1.375- μm MODIS channel to detect thin cirrus clouds during the day time is expected to be one to two orders of magnitude better than the current infrared emission techniques. As a result, a larger fraction of the satellite data will likely be identified as containing cirrus clouds. In order to make better studies of surface reflectance properties, thin cirrus effects must be removed from satellite images. We have developed an empirical approach for removing/correcting thin cirrus effects in the 0.4 - 1.0 μm region using channels near 1.375 μm . This algorithm will be incorporated into the present MODIS atmospheric correction algorithms for ocean color and land applications and will yield improved MODIS atmospheric aerosol, land surface, and ocean color products.

2. BACKGROUND

Because of their partial transparency, thin cirrus clouds are difficult to detect in satellite images, particularly over land, both in the visible and in the 10–12 μm IR atmospheric window regions (Rossow et al., 1985). In order to illustrate the semi-transparent nature of thin cirrus clouds, we show in Figure 1 examples of images acquired with the Airborne Visible Infrared Imaging Spectrometer (AVIRIS) from an ER-2 aircraft at 20 km altitude during the NASA-sponsored First International Satellite Cloud Climatology Project Experiment Phase II Cirrus program (hereinafter FIRE II; cf. Starr et al., 1990) over Coffeyville in southeastern Kansas in December of 1991. From the 0.65- μm image in Fig. 1a, the streets of Coffeyville (in the upper right portion of the image), roads, and various surface fields, are clearly seen. Cirrus clouds are not obviously seen in this image. The 1.38- μm image in Fig. 1b shows only the upper level thin cirrus clouds; the surface features are not seen because atmospheric water vapor below the cirrus clouds completely absorbs the 1.38 μm sunlight. As a result, the 1.38- μm AVIRIS channel detected only the solar radiation scattered by the cirrus clouds. Without the 1.38- μm image, one would not know that the 0.65- μm image was contaminated by thin cirrus clouds. This same problem has affected all satellites used for land and ocean remote sensing; quantification of cirrus effects was not possible because of the lack of appropriate channels to detect thin cirrus clouds.

Based on the observation from AVIRIS data that narrow channels near the center of the strong 1.38- μm water vapor band are very effective in detecting thin cirrus clouds (Gao et al., 1993), Gao and Kaufman (1995) proposed to put a channel centered at 1.375 μm with a width of 30 nm on MODIS for detecting thin cirrus clouds from space. With strong support from the MODIS Science Team members and NASA Goddard Space Flight

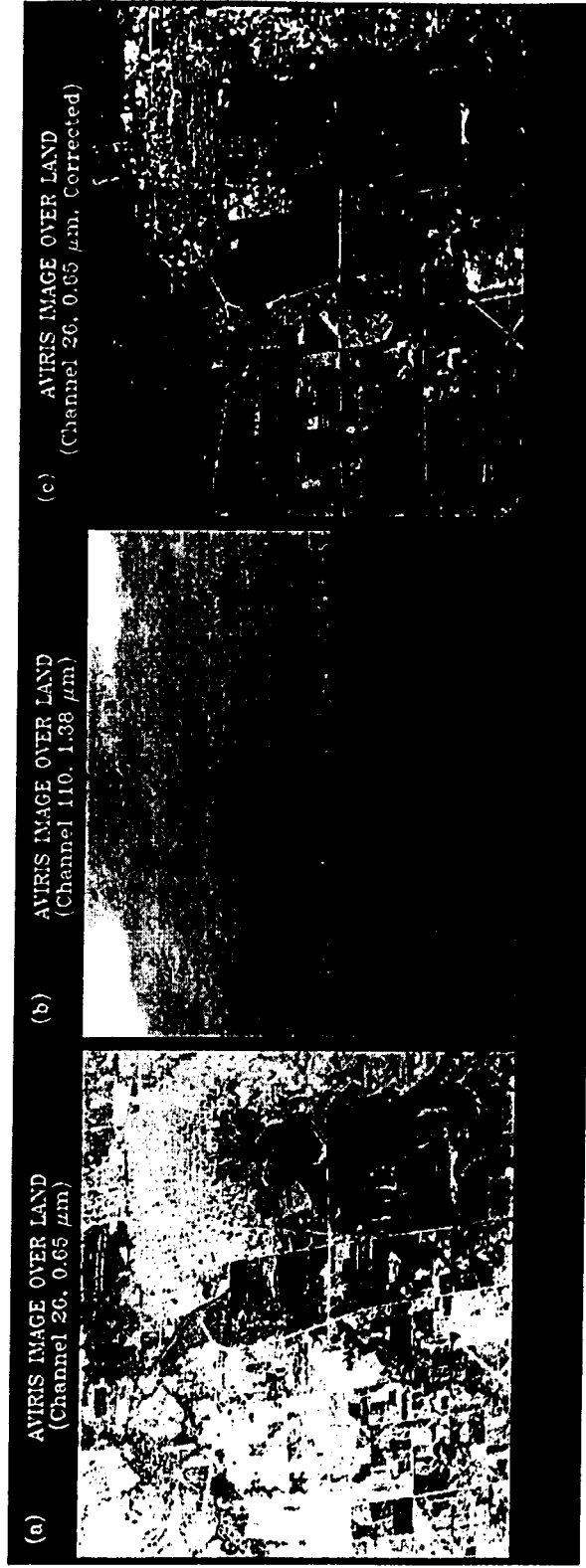


Fig. 1. AVIRIS 0.65 μm image (a), 1.38 μm image (b), and cirrus path radiance corrected 0.65 μm image (c) over Coffeyville in southeastern Kansas. The AVIRIS data were acquired on December 5, 1991.

Center management, the proposed channel was implemented on the MODIS instruments (Salomonson et al., 1989; King et al., 1992; Asrar and Greenstone, 1995) to be flown on the Earth Observing System (EOS) (Butler et al., 1987) AM and PM Platforms. The sensitivity of the 1.375- μm MODIS channel to detect thin cirrus clouds during the day time is expected to be one to two orders of magnitude better than the current infrared emission techniques (Gao and Kaufman, 1995). In this paper, we refer to ice clouds with reflectances in the visible spectral region of 0.1 or less as thin cirrus clouds.

In order to make better studies of reflectance properties of land and ocean surfaces, thin cirrus effects must be removed from satellite images. Therefore, there is a need to study radiative properties of thin cirrus clouds, so that a strategy for correction or removal of the thin cirrus effects, similar to the correction of atmospheric aerosol effect (e.g., Kaufman and Sendra, 1988), can be formed. In this paper, we describe an empirical approach for removing/correcting thin cirrus path radiances in AVIRIS images using channels near 1.375 μm .

3. CIRRUS PROPERTIES

Cirrus clouds consist of ice particles having different sizes and shapes. The "effective" particle sizes (radii of equivalent spheres) are usually greater than 5 μm . We illustrate the scattering and absorption properties of cirrus clouds through examples. Figure 2 shows two AVIRIS spectra (in reflectance units) acquired over areas covered by thick and thin cirrus clouds above Monterey Bay in California on September 4, 1992. The MODIS channels are also indicated. For each spectrum, the reflectances of ice particles in the 0.45 - 1.0 μm spectral region are nearly constant with wavelength, because ice particles are much larger than wavelengths and ice is non-absorbing. The larger apparent reflectances in the 0.45 - 0.6 μm region are due to Rayleigh scattering. Past 1.0 μm one finds several ice absorption bands, for example those centered near 1.5 and 2.0 μm . Weak ice absorptions occur near 1.24 μm and 1.375 μm ; the imaginary parts of the ice refractive index are about the same at both wavelengths. The measured reflectances at 1.375 μm are smaller than reflectances in the 0.4–1.0 μm region mainly because of absorption by water vapor above and within the cirrus clouds. These upper-level water vapor absorption effects need to be accounted for before we can use the 1.375- μm channel for quantitative removal of cirrus effects in other channels.

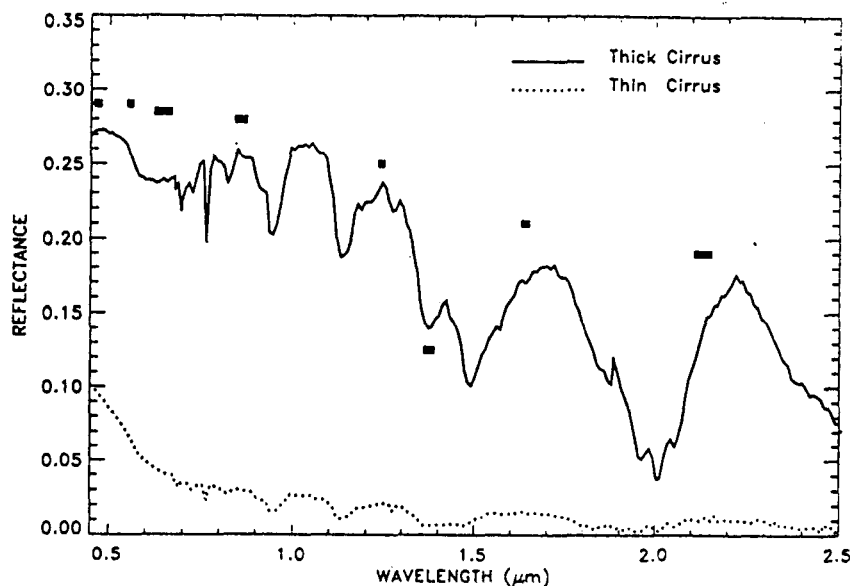


Fig. 2. Examples of AVIRIS spectra over thick and thin cirrus clouds.

At present, our knowledge of cirrus ice particle size, shape, and orientation distributions, spatial variability, and scattering phase functions is not sufficient for reliable, routine modeling of cirrus reflectivity (King, 1993; Shiobara and Asano, 1994). Cirrus spatial inhomogeneity and adjacency effects are difficult to treat properly

in radiative transfer models. In view of these difficulties, we have decided to use empirical relationships to characterize the main cirrus properties, and from these to develop an empirical cirrus removal technique.

4. THE EMPIRICAL APPROACH

For thin cirrus clouds, we assume that a homogeneous thin cirrus layer is located above a "virtual surface", which includes the effects of Rayleigh scattering and land or ocean surface reflection and scattering. Omitting for convenience the wavelength (λ) and cosine-solar-zenith-angle (μ_0) dependencies, we denote the "apparent reflectance" at the satellite as

$$\rho^* = (\pi L / \mu_0 E_0)$$

where L is the radiance measured by the satellite and E_0 is the extra-terrestrial solar flux. Then, accounting for transmission through the cirrus cloud and multiple reflections between cloud and the "virtual surface", we have the following relationship (similar to what is done for aerosol correction, e.g., Fraser and Kaufman, 1985):

$$\rho^* = \rho_0 + T_c \rho / (1 - S_c \rho) \quad (1)$$

where ρ_c is the reflectance of the cirrus cloud, T_c is the two-way transmission (direct + diffuse) through the cloud, ρ is the reflectance of the "virtual surface", and S_c is the cloud-base reflectance of upward radiation. Because $S_c \rho \ll 1$ for thin cirrus, Eq. (1) can be simplified to:

$$\rho^* = \rho_c + T_c \rho \quad (2)$$

In order to remove the cirrus effect from the satellite measurement ρ^* , namely to derive ρ based on (2), cirrus reflectance ρ_c and transmittance T_c must be known.

Analyzing AVIRIS data, we have found that cirrus reflectance ρ_c for AVIRIS channels between 0.4 and 1.0 μm is linearly related to ρ_c at 1.375 μm , i.e.,

$$\rho_c(\lambda) = \rho_c(1.375 \mu\text{m}) / K_a, \quad 0.4 < \lambda < 1.0 \mu\text{m} \quad (3)$$

where K_a is an empirical parameter derived from AVIRIS data themselves. It is essentially the 1.375- μm channel transmittance for water vapor above and within cirrus clouds. The weak ice absorption at 1.375 μm (see Fig. 2) also decreases slightly the K_a value. Substituting (3) into (2), we obtain:

$$T_c \rho = \rho^* - \rho_c(1.375 \mu\text{m}) / K_a, \quad 0.4 < \lambda < 1.0 \mu\text{m} \quad (4)$$

The image of $T_c \rho$ is referred to as the "cirrus-path-radiance-corrected" image in this paper. It is similar to the "virture surface" reflectance image of ρ because of the large transmittances of thin cirrus (T_c is usually greater than 0.9).

5. RESULTS

The technique described by Eq. (4) for removing cirrus path radiances, i.e, to derive images of $T_c \rho$, has been applied to several AVIRIS data sets acquired over different geographical regions during various NASA sponsored field programs. Results from AVIRIS data measured over the Gulf of Mexico, and over Coffeyville in southeastern Kansas are described below.

5.1 The Gulf of Mexico

AVIRIS data were acquired over the Gulf of Mexico on December 5, 1991 during the FIRE Phase II Cirrus Field Program. Figure 3a shows the 0.86- μm AVIRIS image, which reveals both the upper level extended cirrus clouds and the lower level cumulus clouds. Figure 3b shows the 1.38- μm image. Only the upper level cirrus clouds are seen in this image. Figure 4 shows the scatter plot of ρ^* (1.38 μm) versus ρ^* (1.24 μm) for all pixels in

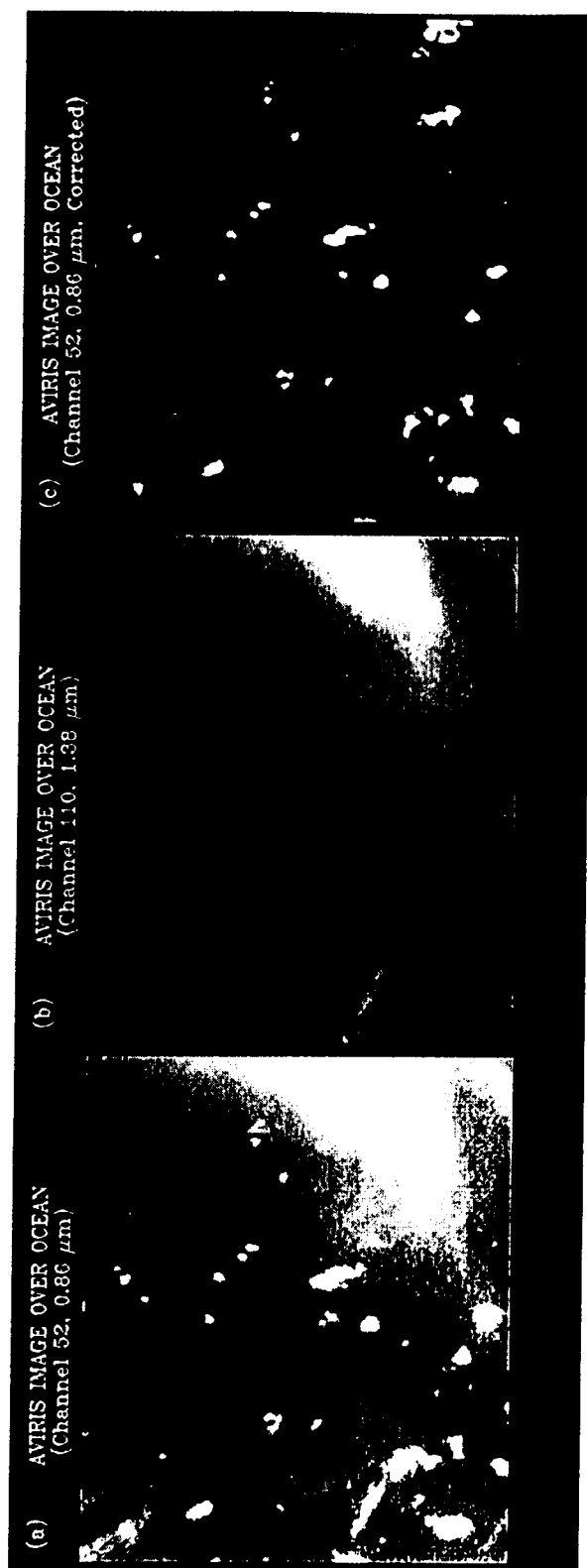


Fig. 3. AVIRIS 0.86 μm image (a), 1.38 μm image (b), and cirrus path radiance corrected 0.86 μm image (c) over the Gulf of Mexico. The AVIRIS data were acquired on December 5, 1991.

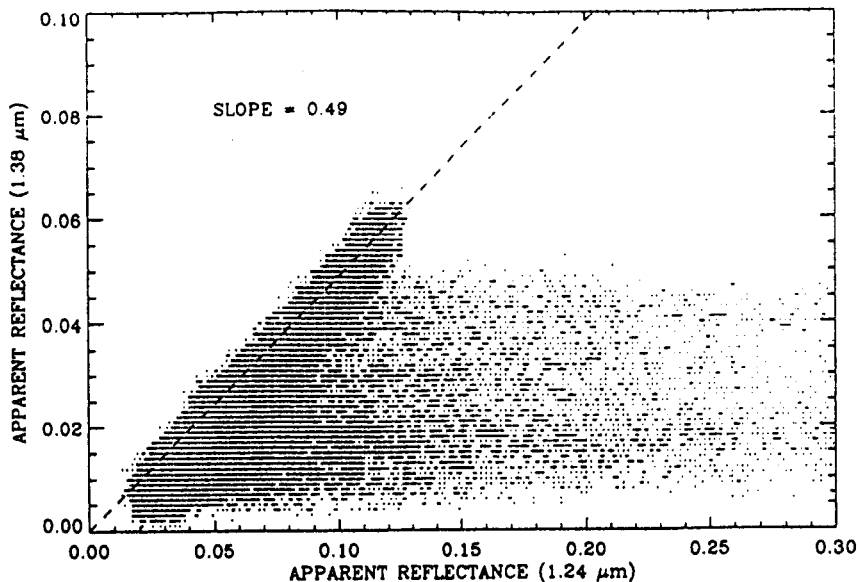


Fig. 4. A scatter plot of apparent reflectances at 1.38 μm versus those at 1.24 μm for the Gulf of Mexico scene.

the scene. We have found that the pixels covered by the upper level thin cirrus clouds are clustered around a straight line with a slope of 0.49 (see the dashed line). This slope is a good estimation of K_a (see Eq. (3)). Because cumulus clouds have higher reflectances at 1.24 μm and are invisible at 1.38 μm , the pixels containing both upper level cirrus and lower level cumulus are spread out to the right of the dashed line. Using the estimated K_a and based on Eq. (4), we have obtained a "cirrus-path-radiance-corrected" image, $T_c\rho$, which is shown in Figure 3c. Cirrus clouds are mostly removed while the cumulus clouds are still present in this image.

In order to have more quantitative descriptions of our cirrus removals, we show in Figure 5 several histograms for pixel reflectances. Fig. 5a shows this for the 0.86- μm image in Fig. 3a. The long tail to the right is typical of most cloudy images. Fig. 5b shows the histogram of the 1.38- μm image; the peak occurs at an "apparent" reflectance value of about 0.012. The maximum "apparent" reflectance value is approximately 0.06. These indicate that the cirrus clouds in the scene (see Fig. 3b) are very thin. The histogram also shows that there are almost no pixels with zero reflectances. Therefore, the entire scene is filled by thin cirrus. Fig. 5c shows the histogram of the "cirrus-path-radiance-corrected" 0.86- μm image, which peaks at a reflectance value of approximately 0.023. This value is what one would normally expect for the specular and waving water surfaces under clear conditions. At 0.86 μm , there is no upwelling radiance from beneath the air-water interface because of the strong sea water absorption of solar radiation. The histogram in Fig. 5c is similar to a gaussian curve, except for a long tail to the right due to small amounts of cumulus clouds in the scene (see Fig. 3c). When random noises are present in the measurements, the histogram for clear ocean pixels should follow a gaussian distribution. Therefore, the histogram in Fig. 5c indicates that our cirrus removal algorithm works reasonably well in this case.

5.2 Coffeyville, Kansas

AVIRIS data was acquired over Coffeyville in southeastern Kansas on December 5, 1991 during the FIRE Phase II Cirrus Program. The images of the 0.65 and 1.38 μm channels were shown in Figures 1a and 1b, respectively. The two bright areas in the upper left and upper right portions of Fig. 1b have apparent reflectance values between 0.05 and 0.06, indicating thin cirrus. The corresponding areas in Fig. 1a appear more blurred than the other areas covered by thinner clouds.

In order to use the 1.38- μm image for quantitative corrections of thin cirrus effects in the 0.65- μm image, we have to estimate the upper level water vapor transmittance, K_a (see Eq. 3). Because the land surface reflectances at 1.24 μm are quite variable spatially, the scatter plot method $\rho(1.38 \mu\text{m})$ versus $\rho(1.24 \mu\text{m})$ for the estimation of

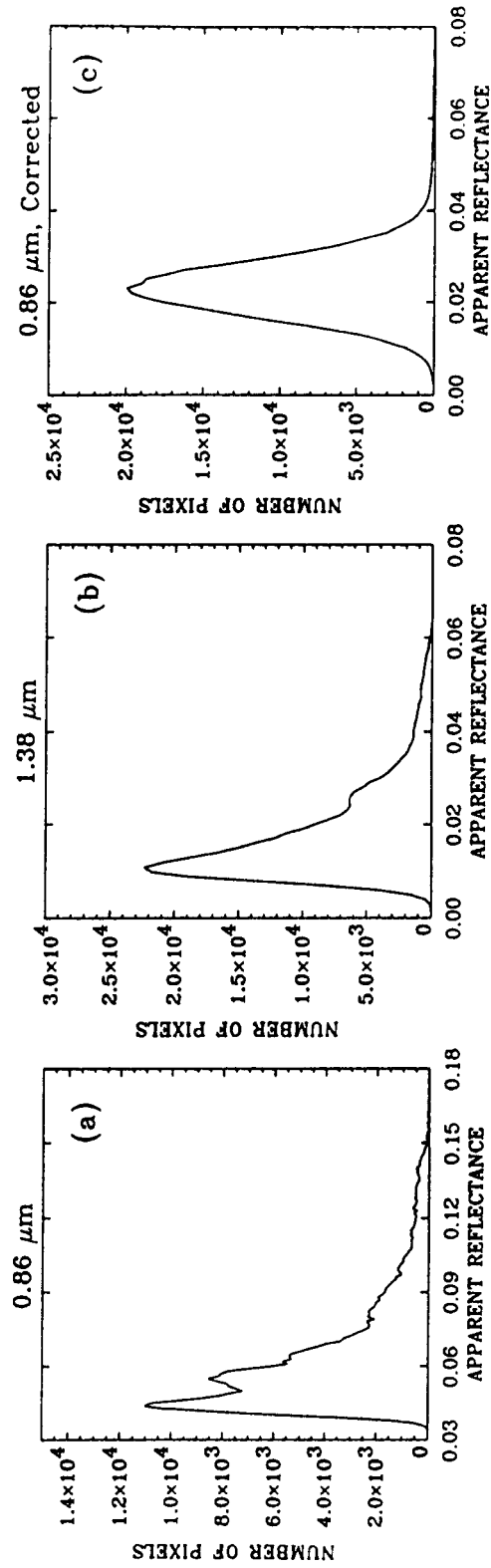


Fig. 5. Histograms corresponding to the 0.86 μm image (a), 1.38 μm image (b), and cirrus path radiance corrected 0.86 μm image (c) in Fig. 3.

K_a over water surfaces is not directly applicable to the land. Since green vegetation in the 0.64 - 0.67 μm spectral region has low and spatially uniform reflectances (~ 0.03), we used the scatter plot of $\rho(1.38 \mu\text{m})$ versus $\rho(0.65 \mu\text{m})$ for pixels covered by green vegetation (mainly winter wheat) in the estimation of K_a . The vegetated pixels are dark in Fig. 1a. The green vegetation pixels we used in the scatter plot have values of NDVI (the normalized difference vegetation index defined as $(\rho_{0.86 \mu\text{m}}^* - \rho_{0.65 \mu\text{m}}^*) / (\rho_{0.86 \mu\text{m}}^* + \rho_{0.65 \mu\text{m}}^*)$) of 0.43 or greater. The estimated K_a is 0.7. Fig. 1c shows the path-radiance-corrected 0.65- μm image using this value of K_a . Surface features, particularly those in the upper left and upper right portions, are less blurred than those in Fig. 1a.

6. DISCUSSIONS

There are two kinds of errors introduced in our correction of cirrus path radiance effects in the 0.4 - 1.0 μm region. One kind of error is due to uncertainty in the estimated coefficient K_a from imaging data themselves. The other kind of error is the lack of correction for the cirrus transmittance factor, T_c . We expect that the combined errors introduced are smaller for thin cirrus over the dark ocean areas than for thick cirrus over brighter land areas.

Accurate corrections for the cirrus transmittances T_c in the 0.4 - 1.0 μm region are, in practice, more difficult than the corrections of path radiances. Because cirrus clouds are high in the atmosphere (typically 6 - 16 km above the sea level), the solar radiation on the two-way path (Sun-cirrus-surface-cirrus-sensor) encounters cirrus clouds at different spatial locations. If cirrus clouds are thick and their spatial distributions are not uniform, it is difficult to derive T_c from imaging data themselves due to the non-local nature of T_c . However, if cirrus clouds are thin and uniform, T_c can be considered to be equal to $[1 - \rho_c(1.375 \mu\text{m}) / K_a]^n$, where n is a parameter with typical values in the range between 1 and 2. n depends on both the solar and view geometries. For the situation of thin cirrus clouds over the dark ocean, n should be close to 1. So far, we haven't found a reliable method to obtain n and therefore T_c from imaging data themselves for images acquired over land.

7. SUMMARY

We have developed an empirical technique that is successful in removing the cirrus path radiances in AVIRIS images between 0.4 and 1.0 μm . The same technique is being incorporated into the present MODIS atmospheric correction algorithms for ocean color and land applications and will yield improved MODIS atmospheric aerosol, land surface, and ocean color products.

8. ACKNOWLEDGMENTS

The authors are grateful to R. O. Green of Jet Propulsion Laboratory for providing AVIRIS data used in this study, and to A. F. H. Goetz at Department of Geological Sciences, University of Colorado at Boulder for useful discussions on radiative properties of thin cirrus clouds. This research is partially supported by a contract from NASA/Goddard Space Flight Center in Greenbelt, Maryland to Naval Research Laboratory in Washington, DC.

9. REFERENCES

- Asrar, G., R. Greenstone, (Editors), 1995: Mission to planet earth/earth observing system reference handbook, National Aeronautics and Space Administration, Goddard Space Flight Center, Mail Code 900, Greenbelt, MD 20771, USA, 277p.
- Butler, D. M., et al., 1987, From pattern to process: The strategy of the earth observing system, in NASA Earth Observing System, Vol II, pp. 1-29, NASA, Washington D.C.
- Fraser, R.S. and Y.J. Kaufman, 1985: 'The relative importance of aerosol scattering and absorption in remote sensing', *IEEE Trans. Geosc. Rem. Sens.*, **GE-23**, 525-633.
- Gao, B.-C., A. F. H. Goetz, and W. J. Wiscombe, 1993, Cirrus cloud detection from airborne imaging spectrometer data using the 1.38 μm water vapor band, *Geophys. Res. Lett.*, **20**, 301-304.
- Gao, B.-C., and Y. J. Kaufman, 1995, Selection of the 1.375- μm MODIS channel for remote sensing of cirrus clouds and stratospheric aerosols from space, *J. Atm. Sci.*, **52**, 4231-4237.
- Kaufman, Y.J. and C. Sendra, 1988: Satellite mapping of aerosol loading over vegetated areas. Ed. P. V. Hobbs and M. P. McCormick, *Aerosols and Climate*, A. Deepak Publ., Hampton, VA., 51-67.

- King, M. D., Y. J. Kaufman, W. P. Menzel, and D. Tanre, 1992, Remote sensing of cloud, aerosol and water vapor properties from the Moderate Resolution Imaging Spectrometer (MODIS), *IEEE Trans. Geosci. Remote Sens.*, 30, 2-27.
- King, M. D., 1993, Radiative Properties of Clouds, in *Aerosol-Cloud-Climate Interactions*, (P. Hobbs editor), Academic Press, 123-149.
- Rossow, W. B., F. Moshier, E. Kinsella, A. Arking, M. Desbois, E. Harrison, P. Minnis, E. Ruprecht, G. Seze, C. Simmer, and E. Smith, 1985, ISCCP cloud algorithm intercomparison, *J. Clim. Appl. Meteorol.*, 24, 877-903.
- Salomonson, V. V., W. L. Barnes, P. W. Maymon, H. E. Montgomery, and H. Ostrow, 1989, MODIS: Advanced facility instrument for studies of the earth as a system, *IEEE Trans. Geosci. Remote Sens.*, 27, 145-153.
- Shiobara, M., T. Hayasaka, T. Nakajima, and M. Tanaka, 1991, Aerosol monitoring using a scanning spectral radiometer in Sendai, Japan, *J. Meteorol. Soc. Japan*, 69, 57-70.
- Starr, D. O'C., et al., 1990, FIRE Phase II: Cirrus Implementation Plan, can be obtained from the FIRE Project Office at NASA Langley Research Center in Hampton, Virginia.
- Vane, G., R.O. Green, T.G. Chrien, H.T. Enmark, E.G. Hansen, and W.M. Porter, 1993, The Airborne Visible Infrared Imaging Spectrometer, *Remote Sens. Env.*, 44(2/3), 127-143.